PHYSICAL REVIEW C **82**, 034909 (2010)

Parton energy loss in heavy-ion collisions via direct-photon and charged-particle azimuthal correlations

B. I. Abelev,[8] M. M. Aggarwal,[30] Z. Ahammed,[47] A. V. Alakhverdyants,[17] B. D. Anderson,[18] D. Arkhipkin,[3] G. S. Averichev,[17] J. Balewski,[22] O. Barannikova,[8] L. S. Barnby,[2] J. Baudot,[15] S. Baumgart,[52] D. R. Beavis,[3] R. Bellwied,[50] F. Benedosso,[27] M. J. Betancourt,[22] R. R. Betts,[8] A. Bhasin,[16] A. K. Bhati,[30] H. Bichsel,[49] J. Bielcik,[10] J. Bielcikova,[11] B. Biritz,[6] L. C. Bland,[3] I. Bnzarov,[17] M. Bombara,[2] B. E. Bonner,[36] J. Bouchet,[18] E. Braidot,[27] A. V. Brandin,[25] E. Bruna,[52] S. Bueltmann,[29] T. P. Burton,[2] M. Bystersky,[11] X. Z. Cai,[40] H. Caines,[52] M. Calderón de la Barca Sánchez,[5] O. Catu,[52] D. Cebra,[5] R. Cendejas,[6] M. C. Cervantes,[42] Z. Chajecki,[28] P. Chaloupka,[11] S. Chattopadhyay,[47] H. F. Chen,[38] J. H. Chen,[18] J. Y. Chen,[51] J. Cheng,[44] M. Cherney,[9] A. Chikanian,[52] K. E. Choi,[34] W. Christie,[3] R. F. Clarke,[42] M. J. M. Codrington,[42] R. Corliss,[22] T. M. Cormier,[50] M. R. Cosentino,[37] J. G. Cramer,[49] H. J. Crawford,[4] D. Das,[5] S. Dash,[12] M. Daugherity,[43] L. C. De Silva,[50] T. G. Dedovich,[17] M. DePhillips,[3] A. A. Derevschikov,[32] R. Derradi de Souza,[7] L. Didenko,[3] P. Djawotho,[42] S. M. Dogra,[16] X. Dong,[21] J. L. Drachenberg,[42] J. E. Draper,[5] J. C. Dunlop,[3] M. R. Dutta Mazumdar,[47] L. G. Efimov,[17] E. Elhalhuli,[2] M. Elnimr,[50] J. Engelage,[4] G. Eppley,[36] B. Erazmus,[41] M. Estienne,[41] L. Eun,[31] P. Fachini,[3] R. Fatemi,[19] J. Fedorisin,[17] A. Feng,[51] P. Filip,[17] E. Finch,[52] V. Fine,[3] Y. Fisyak,[3] C. A. Gagliardi,[42] L. Gaillard,[2] D. R. Gangadharan,[6] M. S. Ganti,[47] E. J. Garcia-Solis,[8] A. Geromitsos,[41] F. Geurts,[36] V. Ghazikhanian,[6] P. Ghosh,[47] Y. N. Gorbunov,[9] A. Gordon,[3] O. Grebenyuk,[21] D. Grosnick,[46] B. Grube,[34] S. M. Guertin,[6] K. S. F. F. Guimaraes,[37] A. Gupta,[16] N. Gupta,[16] W. Guryn,[3] B. Haag,[5] T. J. Hallman,[3] A. Hamed,[42] J. W. Harris,[52] W. He,[14] M. Heinz,[52] S. Heppelmann,[31] B. Hippolyte,[15] A. Hirsch,[33] E. Hjort,[21] A. M. Hoffman,[22] G. W. Hoffmann,[43] D. J. Hofman,[8] R. S. Hollis,[8] H. Z. Huang,[6] T. J. Humanic,[28] L. Huo,[42] G. Igo,[6] A. Iordanova,[8] P. Jacobs,[21] W. W. Jacobs,[14] P. Jakl,[11] C. Jena,[12] F. Jin,[40] C. L. Jones,[22] P. G. Jones,[2] J. Joseph,[18] E. G. Judd,[4] S. Kabana,[41] K. Kajimoto,[43] K. Kang,[44] J. Kapitan,[11] K. Kauder,[8] D. Keane,[18] A. Kechechyan,[17] D. Kettler,[49] V. Yu. Khodyrev,[32] D. P. Kikola,[21] J. Kiryluk,[21] A. Kisiel,[48] S. R. Klein,[21] A. G. Knospe,[52] A. Kocoloski,[22] D. D. Koetke,[46] J. Konzer,[33] M. Kopytine,[18] I. Koralt,[29] W. Korsch,[19] L. Kotchenda,[25] V. Kouchpil,[11] P. Kravtsov,[25] V. I. Kravtsov,[32] K. Krueger,[1] M. Krus,[10] C. Kuhn,[15] L. Kumar,[30] P. Kurnadi,[6] M. A. C. Lamont,[3] J. M. Landgraf,[3] S. LaPointe,[50] J. Lauret,[3] A. Lebedev,[3] R. Lednicky,[17] C-H. Lee,[34] J. H. Lee,[3] W. Leight,[22] M. J. LeVine,[3] C. Li,[38] N. Li,[51] Y. Li,[44] G. Lin,[52] S. J. Lindenbaum,[26] M. A. Lisa,[28] F. Liu,[51] H. Liu,[5] J. Liu,[36] L. Liu,[51] T. Ljubicic,[3] W. J. Llope,[36] R. S. Longacre,[3] W. A. Love,[3] Y. Lu,[38] T. Ludlam,[3] G. L. Ma,[40] Y. G. Ma,[40] D. P. Mahapatra,[12] R. Majka,[52] O. I. Mall,[5] L. K. Mangotra,[16] R. Manweiler,[46] S. Margetis,[18] C. Markert,[43] H. Masui,[21] H. S. Matis,[21] Yu. A. Matulenko,[32] D. McDonald,[36] T. S. McShane,[9] A. Meschanin,[32] R. Milner,[22] N. G. Minaev,[32] S. Mioduszewski,[42] A. Mischke,[27] B. Mohanty,[47] D. A. Morozov,[32] M. G. Munhoz,[37] B. K. Nandi,[13] C. Nattrass,[52] T. K. Nayak,[47] J. M. Nelson,[2] P. K. Netrakanti,[33] M. J. Ng,[4] L. V. Nogach,[32] S. B. Nurushev,[32] G. Odyniec,[21] A. Ogawa,[3] H. Okada,[3] V. Okorokov,[25] D. Olson,[21] M. Pachr,[10] B. S. Page,[14] S. K. Pal,[47] Y. Pandit,[18] Y. Panebratsev,[17] T. Pawlak,[48] T. Peitzmann,[27] V. Perevoztchikov,[3] C. Perkins,[4] W. Peryt,[48] S. C. Phatak,[12] P. Pile,[3] M. Planinic,[53] M. A. Ploskon,[21] J. Pluta,[48] D. Plyku,[29] N. Poljak,[53] A. M. Poskanzer,[21] B. V. K. S. Potukuchi,[16] D. Prindle,[49] C. Pruneau,[50] N. K. Pruthi,[30] P. R. Pujahari,[13] J. Putschke,[52] R. Raniwala,[35] S. Raniwala,[35] R. L. Ray,[43] R. Redwine,[22] R. Reed,[5] A. Ridiger,[25] H. G. Ritter,[21] J. B. Roberts,[36] O. V. Rogachevskiy,[17] J. L. Romero,[5] A. Rose,[21] C. Roy,[41] L. Ruan,[3] M. J. Russcher,[27] R. Sahoo,[41] S. Sakai,[6] I. Sakrejda,[21] T. Sakuma,[22] S. Salur,[21] J. Sandweiss,[52] M. Sarsour,[42] J. Schambach,[43] R. P. Scharenberg,[33] N. Schmitz,[23] J. Seger,[9] I. Selyuzhenkov,[14] P. Seyboth,[23] A. Shabetai,[15] E. Shahaliev,[17] M. Shao,[38] M. Sharma,[50] S. S. Shi,[51] X-H. Shi,[40] E. P. Sichtermann,[21] F. Simon,[23] R. N. Singaraju,[47] M. J. Skoby,[33] N. Smirnov,[52] P. Sorensen,[3] J. Sowinski,[14] H. M. Spinka,[1] B. Srivastava,[33] T. D. S. Stanislaus,[46] D. Staszak,[6] M. Strikhanov,[25] B. Stringfellow,[33] A. A. P. Suaide,[37] M. C. Suarez,[8] N. L. Subba,[18] M. Sumbera,[11] X. M. Sun,[21] Y. Sun,[38] Z. Sun,[20] B. Surrow,[22] T. J. M. Symons,[21] A. Szanto de Toledo,[37] J. Takahashi,[7] A. H. Tang,[3] Z. Tang,[38] L. H. Tarini,[50] T. Tarnowsky,[24] D. Thein,[43] J. H. Thomas,[21] J. Tian,[40] A. R. Timmins,[50] S. Timoshenko,[25] D. Tlusty,[11] M. Tokarev,[17] T. A. Trainor,[49] V. N. Tram,[21] S. Trentalange,[6] R. E. Tribble,[42] O. D. Tsai,[6] J. Ulery,[33] T. Ullrich,[3] D. G. Underwood,[1] G. Van Buren,[3] G. van Nieuwenhuizen,[22] J. A. Vanfossen Jr.,[18] R. Varma,[13] G. M. S. Vasconcelos,[7] A. N. Vasiliev,[32] F. Videbaek,[3] S. E. Vigdor,[14] Y. P. Viyogi,[12] S. Vokal,[17] S. A. Voloshin,[50] M. Wada,[43] M. Walker,[22] F. Wang,[33] G. Wang,[6] H. Wang,[24] J. S. Wang,[20] Q. Wang,[33] X. Wang,[44] X. L. Wang,[38] Y. Wang,[44] G. Webb,[19] J. C. Webb,[46] G. D. Westfall,[24] C. Whitten Jr.,[6] H. Wieman,[21] S. W. Wissink,[14] R. Witt,[45] Y. Wu,[51] W. Xie,[33] N. Xu,[21] Q. H. Xu,[39] Y. Xu,[38] Z. Xu,[3] Y. Yang,[20] P. Yepes,[36] K. Yip,[3] I-K. Yoo,[34] Q. Yue,[44] M. Zawisza,[48] H. Zbroszczyk,[48] W. Zhan,[20] S. Zhang,[40] W. M. Zhang,[18] X. P. Zhang,[21] Y. Zhang,[21] Z. P. Zhang,[38] Y. Zhao,[38] C. Zhong,[40] J. Zhou,[36] X. Zhu,[44] R. Zoulkarneev,[17] Y. Zoulkarneeva,[17] and J. X. Zuo[40]

(STAR Collaboration)

[1]*Argonne National Laboratory, Argonne, Illinois 60439, USA*

[2]*University of Birmingham, Birmingham, United Kingdom*

[3]*Brookhaven National Laboratory, Upton, New York 11973, USA*

[4]*University of California, Berkeley, California 94720, USA*

[5]*University of California, Davis, California 95616, USA*

[6]*University of California, Los Angeles, California 90095, USA*

[7]*Universidade Estadual de Campinas, Sao Paulo, Brazil*

[8]*University of Illinois at Chicago, Chicago, Illinois 60607, USA*

[9]*Creighton University, Omaha, Nebraska 68178, USA*
[10]*Czech Technical University in Prague, FNSPE, Prague, CZ-115 19, Czech Republic*
[11]*Nuclear Physics Institute AS CR, CZ-250 68 Řež/Prague, Czech Republic*
[12]*Institute of Physics, Bhubaneswar 751005, India*
[13]*Indian Institute of Technology, Mumbai, India*
[14]*Indiana University, Bloomington, Indiana 47408, USA*
[15]*Institut de Recherches Subatomiques, Strasbourg, France*
[16]*University of Jammu, Jammu 180001, India*
[17]*Joint Institute for Nuclear Research, Dubna, 141 980, Russia*
[18]*Kent State University, Kent, Ohio 44242, USA*
[19]*University of Kentucky, Lexington, Kentucky, 40506-0055, USA*
[20]*Institute of Modern Physics, Lanzhou, China*
[21]*Lawrence Berkeley National Laboratory, Berkeley, California 94720, USA*
[22]*Massachusetts Institute of Technology, Cambridge, Massachusetts 02139-4307, USA*
[23]*Max-Planck-Institut für Physik, Munich, Germany*
[24]*Michigan State University, East Lansing, Michigan 48824, USA*
[25]*Moscow Engineering Physics Institute, Moscow Russia*
[26]*City College of New York, New York City, New York 10031, USA*
[27]*NIKHEF and Utrecht University, Amsterdam, The Netherlands*
[28]*Ohio State University, Columbus, Ohio 43210, USA*
[29]*Old Dominion University, Norfolk, VA, 23529, USA*
[30]*Panjab University, Chandigarh 160014, India*
[31]*Pennsylvania State University, University Park, Pennsylvania 16802, USA*
[32]*Institute of High Energy Physics, Protvino, Russia*
[33]*Purdue University, West Lafayette, Indiana 47907, USA*
[34]*Pusan National University, Pusan, Republic of Korea*
[35]*University of Rajasthan, Jaipur 302004, India*
[36]*Rice University, Houston, Texas 77251, USA*
[37]*Universidade de Sao Paulo, Sao Paulo, Brazil*
[38]*University of Science & Technology of China, Hefei 230026, China*
[39]*Shandong University, Jinan, Shandong 250100, China*
[40]*Shanghai Institute of Applied Physics, Shanghai 201800, China*
[41]*SUBATECH, Nantes, France*
[42]*Texas A&M University, College Station, Texas 77843, USA*
[43]*University of Texas, Austin, Texas 78712, USA*
[44]*Tsinghua University, Beijing 100084, China*
[45]*United States Naval Academy, Annapolis, Maryland 21402, USA*
[46]*Valparaiso University, Valparaiso, Indiana 46383, USA*
[47]*Variable Energy Cyclotron Centre, Kolkata 700064, India*
[48]*Warsaw University of Technology, Warsaw, Poland*
[49]*University of Washington, Seattle, Washington 98195, USA*
[50]*Wayne State University, Detroit, Michigan 48201, USA*
[51]*Institute of Particle Physics, CCNU (HZNU), Wuhan 430079, China*
[52]*Yale University, New Haven, Connecticut 06520, USA*
[53]*University of Zagreb, Zagreb, HR-10002, Croatia*

(Received 9 December 2009; published 30 September 2010)

Charged-particle spectra associated with direct photon ($\gamma_{\rm dir}$) and π^0 are measured in $p+p$ and Au + Au collisions at center-of-mass energy $\sqrt{s_{NN}} = 200$ GeV with the STAR detector at the Relativistic Heavy Ion Collider. A shower-shape analysis is used to partially discriminate between $\gamma_{\rm dir}$ and π^0. Assuming no associated charged particles in the $\gamma_{\rm dir}$ direction (near side) and small contribution from fragmentation photons ($\gamma_{\rm frag}$), the associated charged-particle yields opposite to $\gamma_{\rm dir}$ (away side) are extracted. In central Au + Au collisions, the charged-particle yields at midrapidity ($|\eta| < 1$) and high transverse momentum ($3 < p_T^{\rm assoc} < 16$ GeV/c) associated with $\gamma_{\rm dir}$ and π^0 ($|\eta| < 0.9$, $8 < p_T^{\rm trig} < 16$ GeV/c) are suppressed by a factor of 3–5 compared with $p+p$ collisions. The observed suppression of the associated charged particles is similar for $\gamma_{\rm dir}$ and π^0 and independent of the $\gamma_{\rm dir}$ energy within uncertainties. These measurements indicate that, in the kinematic range covered and within our current experimental uncertainties, the parton energy loss shows no sensitivity to the parton initial energy, path length, or color charge.

DOI: 10.1103/PhysRevC.82.034909 PACS number(s): 25.75.Bh

I. INTRODUCTION

A major goal of measurements at the Relativistic Heavy Ion Collider (RHIC) is to quantify the properties of the QCD matter created in heavy-ion collisions at high energy [1]. One key property is the medium energy density, which can be probed by its effect on a fast parton propagating through it [2]. A parton scattered in the initial stages of a heavy-ion collision propagates through the medium, in which it may lose energy, and ultimately results in a shower of hadrons (jet), with high transverse momenta (p_T), in the detectors. The medium properties are extracted through the comparison of measured observables with theoretical models. Many perturbative quantum chromodynamics (pQCD)-based models of parton energy loss have successfully described much of the high-p_T data, but the extracted medium parameters span a wide range [3]. In addition to the properties of the medium itself, the amount of energy loss (ΔE) of a parton propagating through the QCD medium can depend on several factors including E, L, C_R, and f, where E is the initial energy of the parton, L is the path length of the parton through the medium, C_R is the Casimir (color charge) factor, and f is the quark flavor (of which the mass can affect the amount of energy loss). To better constrain the medium parameters, it is essential to examine the dependence of ΔE on E, L, and the parton type independently. This necessitates additional experimental observables.

The $\gamma_{\rm dir}$-jet coincidence measurements have long been proposed as a powerful tool for studying parton energy loss in the medium [4]. The leading-order (LO) production processes of direct photons, quark-gluon Compton scattering ($q + g \rightarrow q + \gamma$) and quark-antiquark annihilation ($q + \bar{q} \rightarrow g + \gamma$), are free from the uncertainties accompanying fragmentation. In the LO, the outgoing high-p_T γ balances the p_T of the partner parton separated by π in azimuth ("away-side"), modulo corrections owing to parton intrinsic p_T [5]. The study of the spectra of the away-side jet particles associated with a high-p_T $\gamma_{\rm dir}$ trigger, as a function of $p_T^{\rm trig}$, can constrain the dependence of ΔE on E. The mean-free path of the γ in the medium is large enough that its momentum is preserved, regardless of the position of the initial scattering vertex. The $\gamma_{\rm dir}$ does not suffer from the geometric biases (nonuniform spatial sampling of hadron triggers owing to energy loss in the medium) inherent in dihadron azimuthal correlation measurements. Therefore, it is expected that the away-side parton associated with π^0 loses more energy on average than that associated with $\gamma_{\rm dir}$. A comparison between the spectra of the away-side particles associated with $\gamma_{\rm dir}$ vs π^0 triggers can constrain the dependence of ΔE on L. However, the spectra of the away-side particles associated with $\gamma_{\rm dir}$ and π^0 can be different owing to two additional factors. First, because the Compton scattering is the dominant channel for direct-γ production in the covered phase space, the quark and gluon are present in different proportions opposite to $\gamma_{\rm dir}$ and π^0 triggers, with the away side of the $\gamma_{\rm dir}$ being dominated by quark. In the limit of perturbative interactions with the medium, this would result in the away-side parton associated with π^0 to lose more energy, on average, than that of $\gamma_{\rm dir}$, owing to the bicolored nature of the gluon. Second, the away-side parton associated with π^0 is more energetic than that associated with $\gamma_{\rm dir}$ at the same trigger energy. This is attributable to the fact that the direct γ represents the total scattered constituent momentum while the π^0 represents only a fraction of it. This may or may not result in a difference in energy loss for the away-side parton for the different trigger types, depending on the energy dependence of the energy loss in the medium. While the effects of the color factor and the path-length dependence would both cause the away-side parton associated with π^0 to lose more energy than that associated with $\gamma_{\rm dir}$, the dependence of energy loss on the initial parton energy could, in principle, compensate for these effects. To disentangle the two former effects from the dependence of energy loss on the initial parton energy, one must investigate the dependence of energy loss on $p_T^{\rm trig}$ for $\gamma_{\rm dir}$ triggers.

In this article we examine ΔE by comparing jet yields measured in central Au + Au collisions and $p + p$ collisions at $\sqrt{s_{NN}} = 200$ GeV via correlations in azimuthal angle between high-p_T particles at mid-pseduorapidity. We investigate the ΔE dependence on E, via $\gamma_{\rm dir}$-charged-particle ($\gamma_{\rm dir}$-$h^{\pm}$) correlations as a function of $p_T^{\rm trig}$, and on L (and on C_R), via a comparison of π^0-charged particle (π^0-$h^{\pm}$) to ($\gamma_{\rm dir}$-$h^{\pm}$) correlations. Taking advantage of the unique configuration of the STAR detector, we use a transverse shower-shape analysis to distinguish between π^0 and $\gamma_{\rm dir}$ in a new analysis technique to extract the spectra of charged particles associated with $\gamma_{\rm dir}$. This technique allows for a more statistically significant measurement than that in Ref. [6] of this rare probe.

II. EXPERIMENTAL SETUP AND DATA SETS

The STAR detector is well suited for measuring azimuthal angular correlations owing to the large coverage in pseudorapidity ($|\eta| < 1$) and full coverage in azimuth (ϕ). The barrel electromagnetic calorimeter (BEMC) [7] consists of 4800 channels (towers) and measures the γ energy. The time projection chamber (TPC) [8] detects charged-particle tracks. A crucial part of the analysis is discriminating between showers from $\gamma_{\rm dir}$ and two close γ's from high-p_T π^0 symmetric decays. At $p_T^{\pi^0} \sim 8$ GeV/c, the angular separation between the two γ's resulting from a π^0 decay is typically smaller than a tower size, but a π^0 shower is generally broader than a single γ shower. The barrel shower maximum detector (BSMD) [7] consists of 18 000 channels (strips) in each plane (η and ϕ) and resides at ~5.6 radiation lengths inside the calorimeter towers. The BSMD is capable of $(2\gamma)/(1\gamma)$ separation up to $p_T^{\pi^0} \sim 20$ GeV/c owing to its high granularity. Using the BEMC to select events (i.e., "trigger") with high-p_T γ, the STAR experiment collected an integrated luminosity of 535 μb^{-1} of Au + Au collisions in 2007 and 11 pb^{-1} of $p + p$ collisions in 2006. The Au + Au data are divided into centrality classes based on the uncorrected charged-particle multiplicity in the range $|\eta| < 0.5$ as measured by the TPC. Owing to the bias of the triggered data, around 40% of the Au + Au collisions recorded in this event sample are in the 0%–10% central bin.

III. DATA ANALYSIS

In this analysis, events with vertex within ±55 cm of the center of TPC along the beamline are selected. The BEMC

is calibrated using the 2006 $p + p$ data, using a procedure described elsewhere [9]. The tracking efficiency of charged particles as a function of event multiplicity is determined by embedding $\pi^{\pm}$ in real data. The effects of energy and momentum resolution are estimated to be small compared to other systematic uncertainties in this analysis, and no correction is applied. The charged-track quality criteria are similar to those used in previous STAR analyses [10].

A. Neutral clusters

Events with at least one electromagnetic cluster (defined as one or two towers depending on the relative position of the cluster to the tower's center) with $E_T > 8$ GeV are selected. More than 97% of these clusters have deposited energy greater than 0.5 GeV in each layer of the BSMD. A trigger tower is rejected if it has a track with $p > 3.0$ GeV/c pointing to it, which reduces the number of the electromagnetic clusters by only ∼7%. The remaining neutral clusters are further filtered into π^0 and single γ candidates. The π^0/γ discrimination depends on an analysis of the shower shape, as measured by the BSMD and BEMC.

B. Shower-shape analysis

The shower shape is quantified as the cluster energy, measured by the BEMC, normalized by the position-weighted energy moment, measured by the BSMD strips. The quantity is defined as

$$\frac{E_{\text{cluster}}}{\sum_i e_i r_i^{1.5}}, \tag{1}$$

where the e_i are the BSMD strip energies and r_i are the distances of the strips from the center of the cluster. Wider transverse shower profiles lead to smaller values of this quantity. The exponent on r_i was chosen to optimize the π^0/γ discrimination, based on simulation studies. The shower profile cuts were tuned to obtain a nearly γ_{dir}-free (π^0_{rich}) sample and a sample rich in γ_{dir} (γ_{rich}). Figure 1 shows the probability distribution of the transverse shower-profile quantity for neutral clusters above the trigger threshold of $E_T > 8$ GeV/c, measured in $p + p$ and central Au + Au data, as well as for identified electrons with $E > 4$ GeV. Single photons will have a shower shape similar to the one measured for electrons. The distribution for identified electrons does not change significantly with energy. Above the trigger threshold, most π^0 decays are symmetric and thus reconstructed as a single cluster characterized by a wide transverse shower. This can be seen in the data as the probability distribution of the transverse shower profile quantity is peaked at small values. The central Au + Au data is somewhat less peaked at small values than the $p + p$ data, indicating a larger relative fraction of γ_{dir} owing to the suppression of hadrons at high p_T [11]. The cut for the π^0_{rich} sample is indicated by a vertical line at 0.1, and the rejection power for direct photons (estimated from the identified electron distribution) is 90%. The γ_{rich} sample is selected with a cut of 0.2–0.6 in the transverse shower-profile quantity and contains a mixture of direct photons and contamination from fragmentation photons and photons from asymmetric hadron (π^0 and η) decays. All remaining contamination in the γ_{rich} correlation function is removed subsequently, as described in Sec. IV C.

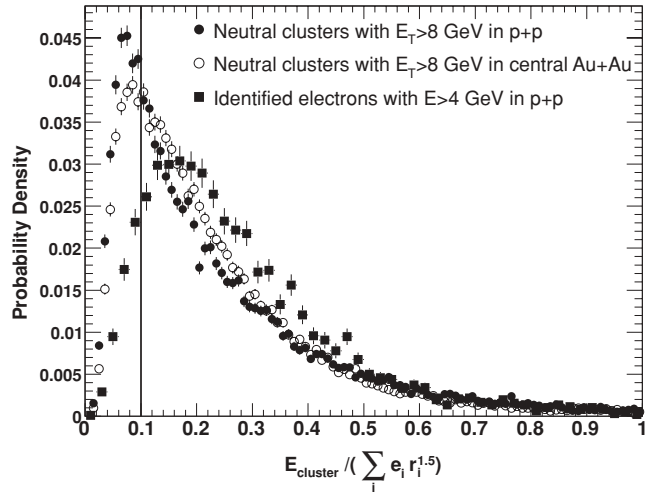

FIG. 1. Probability distributions of the shower-shape quantity [as defined in Eq. (1)] for particles measured as BEMC clusters. The solid circles are neutral clusters above trigger threshold ($E_T > 8$ GeV) in $p + p$ data, the open circles are neutral clusters above trigger threshold in central Au + Au data, and the squares are identified electrons with $E > 4$ GeV. The vertical line is the upper cut value used for identifying π^0.

C. Systematic uncertainties

A detailed study of the shower profile, primary vertex, and charge-rejection cuts is performed to determine the systematic uncertainties, which also include the energy scale uncertainty. The final systematic uncertainties, reported as 1σ errors, are separated into point-to-point systematic errors, which allow the values to vary independently with $z_T = p_T^{\text{assoc}}/p_T^{\text{trig}}$ (or p_T^{trig}), and correlated systematic errors, which require the points to vary together. Additional sources of systematic uncertainties for γ_{dir}-triggered yields are described in Sec. IV C.

D. Azimuthal correlations

The azimuthal correlations, measured as the number of associated particles per trigger per $\Delta\phi$ ("correlation functions"), are used in both $p + p$ and Au + Au collisions to determine the (jet) associated particle yields. Figure 2 shows the correlation functions of charged particles associated with neutral BEMC-cluster triggers for the peripheral (largest impact parameters) and most central (smallest impact parameters) bins in Au + Au collisions for different ranges of p_T^{trig} and p_T^{assoc}. While both near-side ($\Delta\phi \sim 0$) and away-side ($\Delta\phi \sim \pi$) yields increase with trigger energy, the increase on the away side is larger owing to the trigger bias toward high neutral energy. As was previously reported [10] for similar selections in p_T^{trig} and p_T^{assoc}, final-state medium effects cause the away side to be increasingly suppressed with centrality, without significant azimuthal broadening at high-p_T. The suppression of the near-side yield associated with neutral triggers, in central relative to peripheral Au + Au, is consistent with the

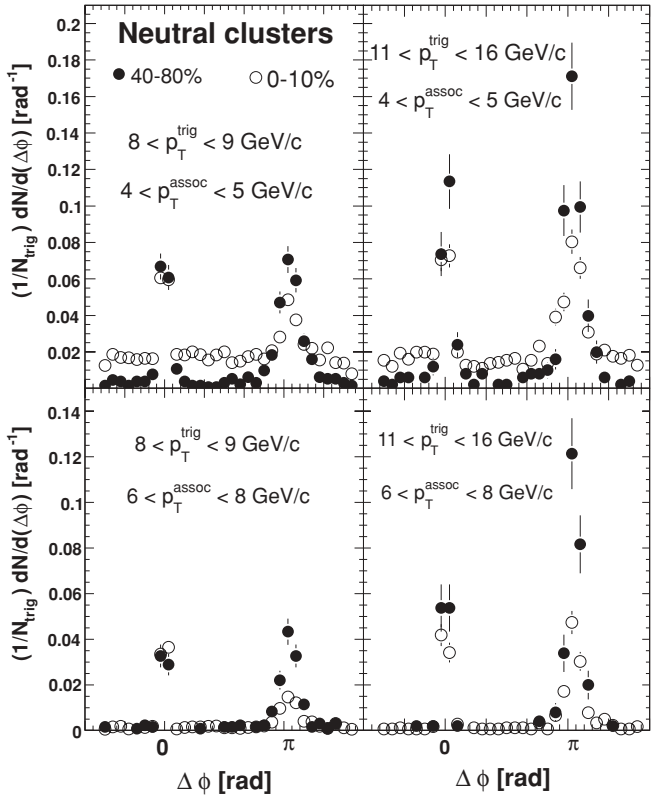

FIG. 2. Correlations (without background subtraction) of neutral-cluster triggers (π^0 and inclusive γ's) with associated charged hadrons measured in central (0%–10%) and peripheral (40%–80%) Au + Au collisions at different bins of $p_T^{\rm trig}$ and $p_T^{\rm assoc}$.

expected increase of the γ/π^0 ratio with centrality at high energy [12].

IV. RESULTS

Figure 3 shows the correlation functions, after applying the shower-shape analysis, for $\gamma_{\rm rich}$ and $\pi^0_{\rm rich}$ triggers for the peripheral and most central bins in Au + Au collisions. As expected, the $\gamma_{\rm rich}$-triggered sample has lower near- and away-side yields than those of the $\pi^0_{\rm rich}$. The nonzero near-side yield for the $\gamma_{\rm rich}$ sample is expected owing to remaining background. The shower-shape analysis is only effective for rejecting two close γ showers, leaving background γ's from asymmetric decays of π^0 and η, and fragmentation γ's.

A. Background subtraction and the extraction of yields

The uncorrelated background level owing to the underlying event is subtracted, assuming an isotropic distribution determined by fitting the correlation function with two Gaussians and a constant. Over the measured range of $p_T^{\rm assoc}$ the expected modulation in the background shape, owing to the correlation with respect to the reaction plane in heavy-ion collisions, is found to have a negligible effect on the subtraction. As shown in Figs. 2 and 3, the level of uncorrelated background is dramatically suppressed relative to the signal and further decreases with increasing $p_T^{\rm assoc}$. The ratio of the pedestal (constant fit value) to the near-side peak height varies from

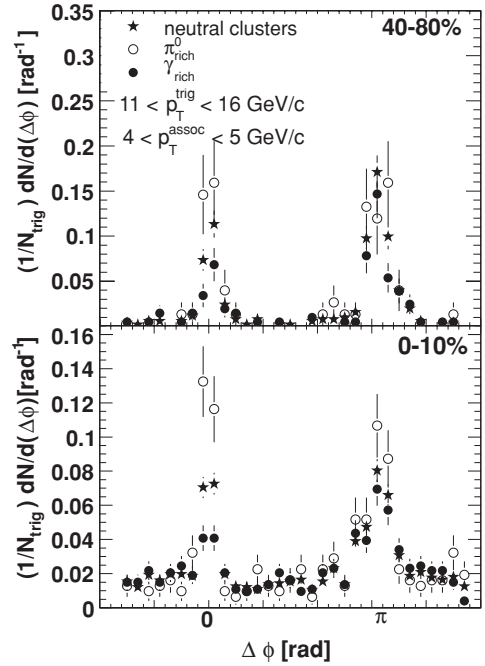

FIG. 3. Correlations (without background subtraction) of neutral-cluster triggers, $\pi^0_{\rm rich}$, and $\gamma_{\rm rich}$ samples with associated charged hadrons measured in peripheral (40%–80%) and central (0%–10%) Au + Au collisions.

0.37 in the lowest reported z_T bin to 0.0081 in the highest in central Au + Au collisions. The near- and away-side yields, Y^n and Y^a, respectively, of associated particles per trigger are extracted by integrating the $(1/N_{\rm trig})\,dN/d(\Delta\phi)$ distributions over $|\Delta\phi| \leqslant 0.63$ and $|\Delta\phi - \pi| \leqslant 0.63$, respectively. The yield is corrected for the tracking efficiency of charged particles as a function of event multiplicity but, as in Ref. [10], not for acceptance owing to the η cuts.

B. Yields associated with π^0 triggers

Figure 4 shows the hadron yields associated with $\pi^0_{\rm rich}$ normalized by the measured number of triggers ($D(z_T)$ [4]), as a function of z_T, compared to the yields per charged-hadron trigger [10]. The left panel shows the near-side yields, and the right panel shows the away-side yields The systematic errors on the $\pi^0_{\rm rich}$-triggered yields have a correlated component of 7%–13%, and point-to-point uncertainties that are typically less than 5%. Because the charged-hadron triggers are dominated by charged pions, the associated yields are expected to be similar to those of π^0 triggers, although there could be some differences owing to the presence of proton triggers in the charged-trigger sample. A general agreement of ∼20%–30% between the $\pi^0 - h^{\pm}$ (this analysis) and the $h^{\pm} - h^{\pm}$ results is clearly seen in both panels of Fig. 4, which further substantiates that the $\pi^0_{\rm rich}$ sample is free of $\gamma_{\rm dir}$.

C. Extraction of $\gamma_{\rm dir}$ associated yields

Assuming zero near-side yield for $\gamma_{\rm dir}$ triggers and a sample of π^0 free of $\gamma_{\rm dir}$, the away-side yield of hadrons correlated

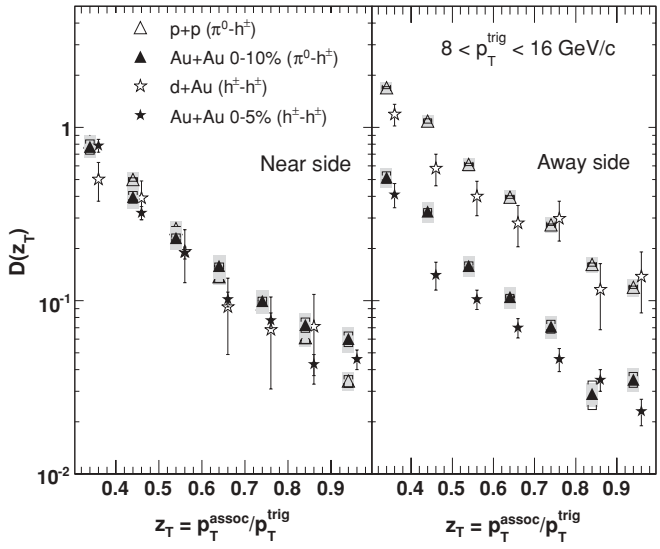

FIG. 4. The z_T dependence of $\pi^0 - h^\pm$ and $h^\pm - h^\pm$ [10] near-side (left panel) and away-side (right panel) associated particle yields. The bin centers are shifted for clarity. The shaded boxes show the systematic errors correlated in z_T, and the brackets show the point-to-point systematic errors.

with the $\gamma_{\rm dir}$ is extracted as

$$Y_{\gamma_{\rm dir}+h} = \frac{Y^a_{\gamma_{\rm rich}+h} - \mathcal{R} Y^a_{\pi^0_{\rm rich}+h}}{1-\mathcal{R}}, \quad \text{where} \quad \mathcal{R} = \frac{Y^n_{\gamma_{\rm rich}+h}}{Y^n_{\pi^0_{\rm rich}+h}}, \quad \text{and} \quad 1-\mathcal{R} = \frac{N^{\gamma_{\rm dir}}}{N^{\gamma_{\rm rich}}}. \tag{2}$$

Here, $Y^{a(n)}_{\gamma_{\rm rich}+h}$ and $Y^{a(n)}_{\pi^0_{\rm rich}+h}$ are the away (near)-side yields of associated particles per $\gamma_{\rm rich}$ and $\pi^0_{\rm rich}$ triggers, respectively. The ratio $\mathcal{R}$ is equivalent to the fraction of "background" triggers in the $\gamma_{\rm rich}$ trigger sample, and $N^{\gamma_{\rm dir}}$ and $N^{\gamma_{\rm rich}}$ are the numbers of $\gamma_{\rm dir}$ and $\gamma_{\rm rich}$ triggers, respectively. The value of $\mathcal{R}$ is found to be ~55% in $p+p$ and decreases to ~30% in central Au + Au with little dependence on $p_T^{\rm trig}$. All background to $\gamma_{\rm dir}$ is subtracted with the assumption that the background triggers have the same correlation function as the $\pi^0_{\rm rich}$ sample. PYTHIA simulations [13] indicate that correlations of γ triggers from asymmetric hadron decays are similar, to within ~10%, to those of symmetrically decaying π^0 triggers as well as the measured correlations of $\pi^0_{\rm rich}$ triggers, at the same $p_T^{\rm trig}$. However, PYTHIA shows that the $\gamma_{\rm frag}$ has a different correlation with the charged particles compared to that of π^0. However, the $\gamma_{\rm frag}$ contribution is expected to fall off more rapidly in x_T ($x_T = 2p_T/\sqrt{s}$) than the other lowest-order $\gamma_{\rm dir}$'s [14]. One theoretical calculation [15] shows the ratio of $\gamma_{\rm frag}$ to $\gamma_{\rm dir}$ to be ~30%–40% at $p_T^\gamma > 8$ GeV/c in $p+p$ at midrapidity at RHIC energy.

For the $\gamma_{\rm dir}$-triggered yields, the systematic errors are evaluated similar to π^0, as described in Sec. III C, and summarized as a function of centrality and z_T in Table I.

An additional source of uncertainty on these yields arises from the assumption that the background contribution of $\gamma_{\rm frag}$ in the $\gamma_{\rm rich}$ triggers has the same correlation as the $\pi^0_{\rm rich}$ triggers and therefore will be subtracted as per Eq. (2). This is assessed by comparing (with a χ^2 analysis) the shape of the near-side correlation of $\gamma_{\rm rich}$ to $\pi^0_{\rm rich}$ triggers. By construction, the near-side yield of $\gamma_{\rm dir}$ integrated over $|\Delta\phi| < 0.63$ is zero. Differences in shape of the near-side correlation of $\gamma_{\rm rich}$ and $\pi^0_{\rm rich}$ triggers can be studied by comparing the bin-by-bin differences (within the bin size) to zero. A χ^2 analysis of such a bin-by-bin comparison is used to calculate the systematic uncertainties associated with the assumption that hadron correlations with $\gamma_{\rm frag}$ triggers are similar to those of the $\pi^0_{\rm rich}$ triggers and therefore subtracted. For $\gamma_{\rm frag}$ which have no near-side yield, such an analysis cannot be performed; and any remaining contamination from such $\gamma_{\rm frag}$ in our $\gamma_{\rm dir}$ sample cannot be assessed.

TABLE I. Systematic errors on $\gamma_{\rm dir}$-triggered yields.

Au + Au 0%–10% collisions z_T-correlated error: 17%–19%						
z_T bin	0.35	0.45	0.55	0.65	0.75	0.85
Point-to-point error (%)	37	21	21	55	20	49
pp collisions z_T-correlated error: 11%–13%						
z_T bin	0.35	0.45	0.55	0.65	0.75	0.85
Point-to-point error (%)	10	13	16	93	17	24

D. Comparison of away-side yields for $\gamma_{\rm dir}$ and π^0 triggers in $p+p$ and Au + Au collisions

Figure 5 shows the z_T dependence of the trigger-normalized away-side yields for $(\pi^0 - h^\pm)$ and $(\gamma - h^\pm)$ in $p+p$ and in 0%–10% central Au + Au collisions. At a given z_T, the away-side yield per π^0 trigger is significantly larger than the yield per $\gamma_{\rm dir}$ trigger. This difference is expected because the $\gamma_{\rm dir}$ carries the total scattered constituent momentum while the π^0 carries only a fraction of it. A comparison to two different theoretical calculations of the associated yields for $\gamma_{\rm dir}$ triggers is shown in Fig. 5. The calculation by Zhang [16] does not include $\gamma_{\rm frag}$ and describes the $p+p$ data well, with a χ^2 per degree of freedom (χ^2/NDF) of 0.2. The χ^2 is calculated taking into account the point-by-point (statistical and systematic) errors only. The calculation by Qin [17] includes a significant contribution of $\gamma_{\rm frag}$, but it is quite similar in yield for $p+p$ and also describes the data, with a χ^2/NDF of 0.5. The away-side $\gamma_{\rm dir}$-triggered yields in Au + Au collisions are also reasonably described by the theoretical calculations, within the current measurement uncertainties, with a χ^2/NDF of 2.8 for the comparison with Zhang and a χ^2/NDF of 1.3 for Qin.

In Au + Au collisions, partonic energy loss can lead to additional differences on the away side because the path length, the energy of the parton, and the partonic species composition of the recoiling parton are different between $\gamma_{\rm dir}$ and π^0 triggers at the same $p_T^{\rm trig}$. To quantify the away-side suppression, we calculate the quantity $I_{\rm AA}$, which is defined as the ratio of the integrated yield of the away-side associated particles per trigger particle in Au + Au to that in $p+p$ collisions. Figures 6 and 7 show $I_{\rm AA}$ as a function of z_T and $p_T^{\rm trig}$, respectively.

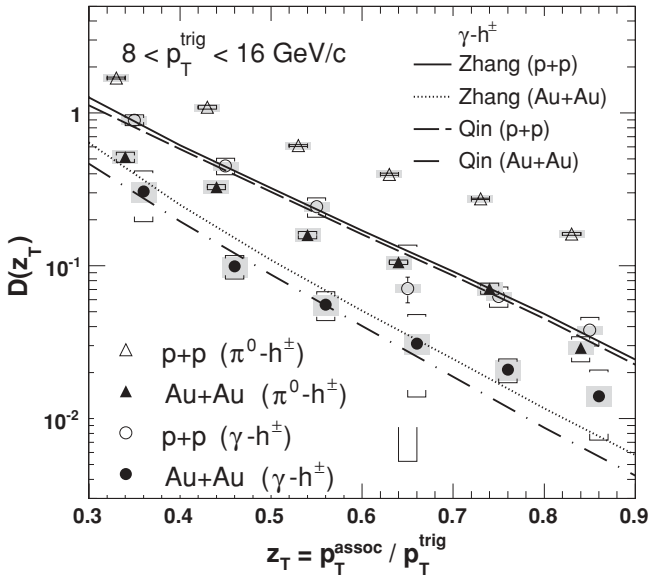

FIG. 5. The z_T dependence of away-side associated-particle yields for π^0 triggers (triangles) and $\gamma_{\rm dir}$ triggers (circles) for $p+p$ (open symbols) and 0%–10% Au + Au (solid symbols) collisions. The trigger particle has $8 < E_T^{\rm trig} < 16$ GeV/c. Boxes show the z_T-correlated systematic errors, and brackets show the point-to-point systematic errors. Data are compared to theoretical calculations. For $p+p$ collisions, the solid line is a calculation by Zhang *et al.* [16] and the dashed line is by Qin *et al.* [17]. For central Au + Au collisions, the dotted line is by Zhang *et al.* [16] and the dash-dotted line is by Qin *et al.* [17].

E. $I_{\rm AA}$ and the ΔE dependence on L and C_R

Despite the differences in yields between $\pi^0 - h^\pm$ and $\gamma - h^\pm$ seen in Fig. 5, Fig. 6 shows that the value of $I_{\rm AA}^{\gamma-h^\pm}$ is z_T independent and similar to that of $I_{\rm AA}^{\pi^0-h^\pm}$. The $I_{\rm AA}^{\gamma-h^\pm}$ agrees

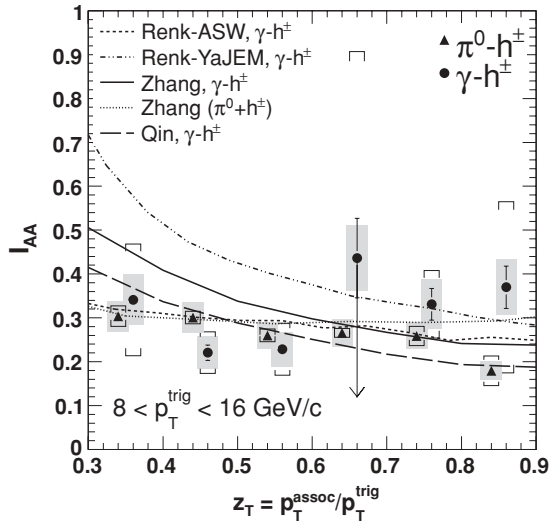

FIG. 6. The z_T dependence of $I_{\rm AA}$ for $\gamma_{\rm dir}$ triggers (circles) and π^0 triggers (triangles). Boxes show the z_T-correlated systematic errors, and brackets show the point-to-point systematic errors. The bin centers are shifted for clarity. Data are compared to theoretical calculations (see text).

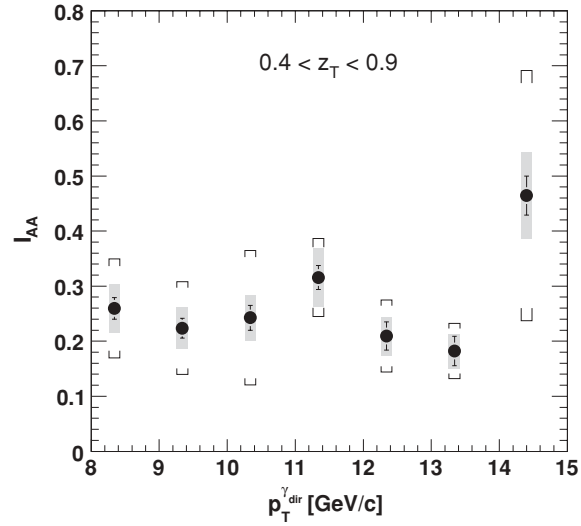

FIG. 7. $I_{\rm AA}$ as a function of p_T for $\gamma_{\rm dir}$ triggers, measured in 0%–10% Au + Au collisions. The associated charged particles have $z_T = 0.4$–0.9. The shaded boxes show the systematic errors correlated in $p_T^{\rm trig}$, and the brackets show the point-to-point systematic errors.

well with theoretical calculations of radiative energy loss that were tuned to the single- and dihadron measurements [10,11]. The calculation by Zhang for both $\gamma_{\rm dir}$ and π^0 triggers [16] shows a small difference in the suppression factor, growing at low z_T. Two calculations for $\gamma_{\rm dir}$ triggers, labeled as Qin [17] and Renk-ASW [18], show even less of a rise at low z_T. In the calculation [18] using the ASW implementation of energy loss [19], the effect of fluctuations in energy loss dominates over the effect of geometry, explaining the similarity in $I_{\rm AA}^{\gamma-h^\pm}$ and $I_{\rm AA}^{\pi^0-h^\pm}$. The calculation that is not consistent with the data at low z_T, the Renk-YaJEM model [18], differs in that the lost energy is tracked and redistributed through the medium. The disagreement with this model may indicate that the lost energy is distributed to extremely low p_T and large angles [18] (as also evidenced by hadron-hadron correlation measurements [20]) and perhaps even that the correlations to the trigger particle are lost. To further test this, one must explore the region of low z_T.

As discussed in Sec. I, a significant dependence of ΔE on L and/or C_R would result in larger average energy loss of the away-side parton for π^0 triggers. In the measured kinematic range, these effects are not observed in the comparison of $I_{\rm AA}^{\gamma-h^\pm}$ and $I_{\rm AA}^{\pi^0-h^\pm}$.

F. $I_{\rm AA}$ and the ΔE dependence on E

The remaining factor that could affect the comparison between $I_{\rm AA}^{\gamma-h^\pm}$ and $I_{\rm AA}^{\pi^0-h^\pm}$ is the dependence of the energy loss on the initial parton energy because $\gamma_{\rm dir}$ triggers carry the same energy as the corresponding away-side parton, while π^0 triggers originate from the fragmentation of a higher-energy parton. Figure 7 addresses the E dependence of ΔE. The suppression of the away-side multiplicity per $\gamma_{\rm dir}$ trigger in Au + Au relative to $p+p$ collisions shows no strong $p_T^{\rm trig}$ dependence, which indicates no strong E dependence in the measured p_T range. This supports the assumption made in

most radiative energy-loss models of no or weak dependence on the initial parton energy [e.g., $\log(E)$,$\sqrt{E}$].

V. SUMMARY

In summary, $\gamma_{\rm dir} - h$ correlation measurements are reported by the STAR collaboration, providing important new constraints on theoretical models. We observed that the level of suppression of hadrons is independent of trigger species (π^0 vs $\gamma_{\rm dir}$) and trigger energy (for $E_T = 8 - 15$ GeV) on the opposite side of the trigger. There are three known factors that could result in differences in the measured $I_{\rm AA}^{\gamma-h^\pm}$ and $I_{\rm AA}^{\pi^0-h^\pm}$: (i) the dependence of energy loss on the initial parton energy, (ii) the energy loss of gluons vs quarks, and (iii) the energy-loss path-length dependence. The measurement of the dependence of $I_{\rm AA}^{\gamma-h^\pm}$ on $p_T^{\rm trig}$ shows no significant dependence on the initial parton energy. The other two factors both result in an expectation of $I_{\rm AA}^{\gamma-h^\pm} > I_{\rm AA}^{\pi^0-h^\pm}$. Thus, the agreement between the measured $I_{\rm AA}^{\gamma-h^\pm}$ and $I_{\rm AA}^{\pi^0-h^\pm}$ in the covered kinematic range indicates that the dependence of observable parton energy loss on parton species and path length traversed by the parton in the medium must be small compared to the experimental uncertainties. This study provides a high-precision cornerstone for more extensive future studies of wider kinematics, identified hadron chemistry, and geometry.

ACKNOWLEDGMENTS

We thank the RHIC Operations Group and RCF at BNL, the NERSC Center at LBNL and the Open Science Grid consortium for providing resources and support. This work was supported in part by the Offices of NP and HEP within the US DOE Office of Science, the US NSF, the Sloan Foundation, the DFG cluster of excellence "Origin and Structure of the Universe," CNRS/IN2P3, STFC and EPSRC of the United Kingdom, FAPESP CNPq of Brazil, Ministry of Education and Science of the Russian Federation, NNSFC, CAS, MoST, and MoE of China, GA and MSMT of the Czech Republic, FOM and NWO of the Netherlands, DAE, DST, and CSIR of India, Polish Ministry of Science and Higher Education, Korea Research Foundation, Ministry of Science, Education, and Sports of the Republic of Croatia, Russian Ministry of Science and Technology, and RosAtom of Russia.

[1] J. Adams *et al.*, Nucl. Phys. A **757**, 102 (2005).
[2] M. Gyulassy, P. Levai, and I. Vitev, Phys. Lett. B **538**, 282 (2002).
[3] S. A. Bass, C. Gale, A. Majumder, C. Nonaka, G. Y. Qin, T. Renk, and J. Ruppert, Phys. Rev. C **79**, 024901 (2009).
[4] X.-N. Wang, Z. Huang, and I. Sarcevic, Phys. Rev. Lett. **77**, 231 (1996).
[5] L. Cormell and J. F. Owens, Phys. Rev. D **22**, 1609 (1980), and references therein.
[6] A. Adare *et al.*, Phys. Rev. C **80**, 024908 (2009).
[7] M. Beddo *et al.*, Nucl. Instrum. Methods A **499**, 725 (2003).
[8] M. Anderson *et al.*, Nucl. Instrum. Methods A **499**, 659 (2003).
[9] B. I. Abelev *et al.*, Phys. Rev. C **81**, 064904 (2010).
[10] J. Adams *et al.*, Phys. Rev. Lett. **97**, 162301 (2006).
[11] S. S. Adler *et al.*, Phys. Rev. Lett. **91**, 072301 (2003).
[12] S. S. Adler *et al.*, Phys. Rev. Lett. **94**, 232301 (2005).
[13] T. Sjöstrand, S. Mrenna, and P. Skands, Comput. Phys. Commun. **178**, 852 (2008) [PYTHIA v8.1].
[14] G. Sterman *et al.*, Rev. Mod. Phys. **67**, 157 (1995).
[15] D. de Florian and W. Vogelsang, Phys. Rev. D **72**, 014014 (2005).
[16] H. Zhang *et al.*, Nucl. Phys. A **830**, 443c (2009).
[17] G.-Y. Qin, J. Ruppert, C. Gale, S. Jeon, and G. D. Moore, Phys. Rev. C **80**, 054909 (2009).
[18] T. Renk, Phys. Rev. C **80**, 014901 (2009).
[19] C. A. Salgado and U. A. Wiedemann, Phys. Rev. D **68**, 014008 (2003).
[20] J. Adams *et al.*, Phys. Rev. Lett. **95**, 152301 (2005); A. Adare *et al.*, Phys. Rev. C **78**, 014901 (2008).